Bulletin of the Geological Society of Finland, Vol. 82, 2010, pp 113–128

# Geochemical and boron isotopic compositions of tourmalines from selected gold-mineralised and barren rocks in SW Finland

MATTI TALIKKA[1] AND SAKU VUORI[2]
[1] *Polar Mining Oy, Käärmesaarentie 3B, FI-02160 Espoo, Finland, matti.talikka@dragonmining.fi*
[2] *Geological Survey of Finland, P.O. Box 96, FI-02151 Espoo, Finland*

## Abstract

Tourmaline-bearing rocks and a number of gold occurrences coexist in southwestern Finland, in a region where extensive magmatism and hydrothermal systems occurred during the Svecofennian orogeny, 1.9–1.8 Ga ago. Tourmalines investigated for this study were sampled from late-orogenic granite pegmatites (Eräjärvi, Kietyönmäki), quartz-tourmaline veins from gold occurrences (Kutemajärvi, Riukka), and the tourmalinised contact between a synorogenic intrusion and supracrustal rocks (Lepomäki Au occurrence, Ylöjärvi Cu-W-As-Ag-Au deposit).

Major element compositions of the tourmalines are controlled by their host lithologies, whereas their boron isotopic compositions reflect the B reservoir(s) and the magmatic-hydrothermal processes of the B-bearing systems. The obtained $\delta^{11}$B values for granite pegmatite, vein, and intrusion-country rock contact-related tourmalines range between -10.2 ‰ and -13.2 ‰, -10.2 ‰ and -11.6 ‰, and -9.6 ‰ and -8.7 ‰, respectively, and are similar to tourmalines worldwide.

The lighter B isotopic composition at Lepomäki gold and Ylöjärvi polymetallic occurrences indicate different B reservoirs and magmatic-hydrothermal processes between syn- and late-orogenic tourmalines. Geological observations and geochemical data on tourmalines also suggest that B was a constituent in hydrothermal fluids at all localities, including the gold-mineralising fluids at Lepomäki, Ylöjärvi and Riukka.

**Keywords**: Tourmaline, Chemical composition, Boron isotopic composition, Gold, Finland.

Editorial handling: Arto Luttinen

## 1. Introduction

Tourmaline may occur in a wide variety of geological settings. As the most widespread B-bearing mineral, tourmaline is an important constituent of the B cycle in earth's crust. Tourmaline is a complex borosilicate with large variations in its chemical and physical properties, and it has a vast pressure-temperature stability range. Hence, tourmaline can be used as an indicator of magmatic, metamorphic, hydrothermal and mineralising processes (e.g. Henry & Guidotti, 1985; Chaussidon & Albarede, 1992; Henry & Dutrow, 1992).

Tourmaline is an important gangue mineral in several metallic and non-metallic ore deposits, for example, in granitoid-related greisens, veins in volcanic and metamorphic rocks, and in stratabound deposits (e.g. Pirajno, 1992; Slack, 1996). The formation of tourmaline is typically related to hydrothermal processes, and the geochemical and B isotopic compositions of tourmalines have been used in the characterisation of hydrothermal fluids and their sources (e.g. Palmer & Slack, 1989; Palmer, 1992; Smith & Yardley, 1996; Jiang et al., 1998).

In the Finnish bedrock, tourmaline is present in a number of mineral occurrences and other geological features. There is, however, a lack of information on the chemical and B isotopic compositions of the Finnish tourmalines. The objective of this study is to produce new geochemical and isotopic data, and consider the processes that are associated with the formation of tourmalines.

## 2. Geologic background

The bedrock of the study area belongs to the Palaeoproterozoic Svecofennian domain that formed as a result of orogenic events 1920–1800 million years ago in the present Finland and Sweden (Lahtinen et al., 2005). The southwestern part of the Finnish Svecofennian domain is characterised by east-west striking supracrustal belts: Tampere, Pirkanmaa, Häme and Uusimaa (Vaasjoki et al., 2005). Sedimentary and volcanic arc igneous rocks and syn- to late-orogenic plutonic rocks are the main constituents in the bedrock of the region (Kähkönen, 2005; Lahtinen et al., 2005). Samples for the present study were collected from six localities in the Tampere and Häme volcano-sedimentary belts in southwestern Finland (Fig. 1).

### 2.1 Tampere Belt

According to Kähkönen (1989; 1999; 2005), Kähkönen and Leveinen (1994), Ojakangas (1986), and Nironen (1989a), the Tampere Belt is predominantly composed of turbiditic metasedimentary rocks, felsic-intermediate arc-type metavolcanic rocks and granitoids, and formed in an island-arc or continental arc setting. The absence of carbonate rocks and iron formations, the presence of turbidites and a mantle reflector dipping to the north indicate a steep convergent plate margin and northward subduction (Kähkönen, 1989; Kähkönen, 1999; Lahtinen et al., 2005). The metasedimentary rocks are mainly 2000–1910 Ma old and the metavolcanic rocks 1904–1889 Ma old (Huhma et al., 1991; Kähkönen et al., 1989; Kähkönen et al., 2004). Synorogenic granitoids in the belt are c. 1.88 Ga old, and the emplacement of the Eräjärvi granite pegmatite cluster is associated with late-orogenic felsic magmatism (Lahti, 1989; Nironen, 1989a). During the Svecofennian orogeny, the supracrustal rocks of the Tampere Belt were deformed and metamorphosed under low-pressure, greenschist to lower amphibolite facies conditions, and the regional metamorphism peaked at c. 1880 Ma (Kilpeläinen, 1998; Mouri et al., 1999).

### 2.2 Häme Belt

The supracrustal rocks of the Häme Belt are divided into two main groups, the older Forssa and the younger Häme Group (Hakkarainen, 1994). The Häme Group is dominated by volcanic rocks, for instance, uralite and plagioclase porphyritic basaltic lavas, and the Forssa Group comprises calc-alkaline volcanic and various clastic sedimentary units (Hakkarainen, 1994). On the basis of their chemical and isotopic compositions, the volcanic rocks of the Forssa Group formed in a relatively mature island-arc and the volcanic rocks of the Häme Group in a rifted-arc setting (Hakkarainen, 1994; Lahtinen, 1996; Kähkönen, 2005). The supracrustal sequence is intruded by 1890–1880 Ma synorogenic intrusions and 1840–1810 Ma late-orogenic microcline granites (Nironen, 2005). In addition to the peak regional metamorphism (1880–1860 Ma) under amphibolite facies conditions, the rocks of the Häme Belt were subjected to a regional high-T event during 1830–1810 Ma that was related to the widespread, late-orogenic microcline granite

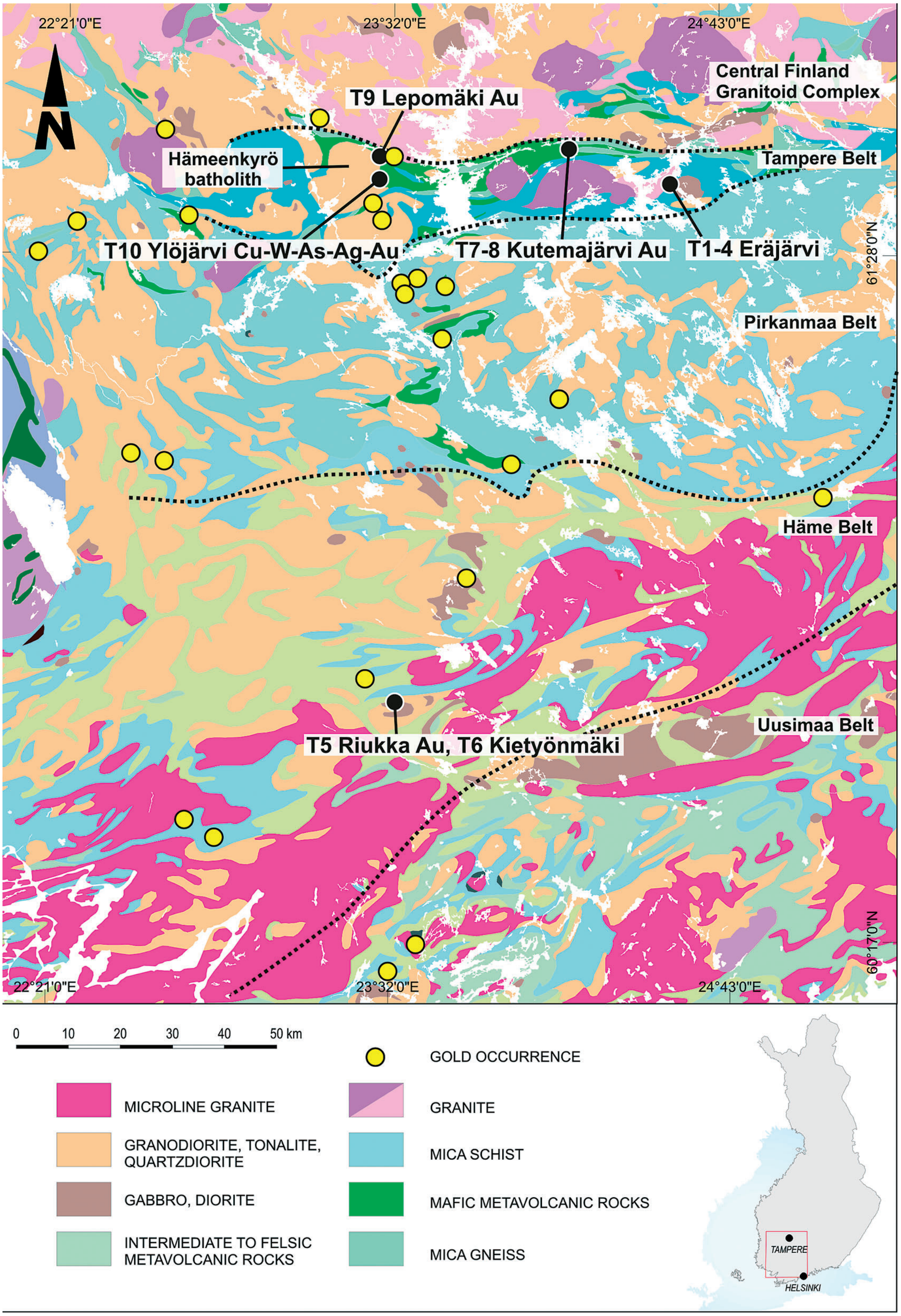

**Fig. 1.** Generalised geological map of the study area in southwestern Finland, showing sample locations and the main geological districts of the region (modified from Korsman et al., 1997; Väisänen et al., 2002).

intrusion and migmatitisation in southern Finland (Väisänen et al., 2002; Kähkönen, 2005).

## 3. Investigated samples

Samples for the present study were selected from different types of tourmaline occurrences representing both gold-mineralised and barren environments. Samples T1–4 and T6 are from granite pegmatites, samples T5 and T7–9 from quartz-tourmaline veins from gold-mineralised rocks, and sample T10 from a tourmaline breccia-hosted Cu-W-As-Ag-Au deposit. More detailed investigations are required to identify variations in geochemical and B isotopic compositions in deposit and/or crystal scale.

### *3.1 Samples T1–4, Eräjärvi pegmatite cluster, Orivesi*

The Eräjärvi pegmatite cluster is located in Orivesi in the eastern part of the volcano-sedimentary Tampere Belt (Fig. 2). Over seventy complex and numerous simple pegmatite or granite pegmatite lenses and dykes are known in the Eräjärvi area (Alviola, 2004). Approximately thirty of the pegmatite deposits have been mined for potassium feldspar and other minerals such as quartz, beryl, muscovite and columbite-tantalite (Lahti, 1981).

The bedrock in the Eräjärvi area mainly comprises metamorphosed and deformed mica schists and plutonic rocks of varying age and composition (Laitakari, 1986). The late-orogenic pegmatites typically occur as lenses or dykes in the supracrustal rocks in the vicinity of granitoid contacts (Lahti, 1989). The emplacement of the pegmatites is associated with felsic magmatism, and the U-Pb dating of metamict zircons from the Viitaniemi and Eräpyhä pegmatites indicate an age of c. 1.8 Ga (Lahti, 1989). Tourmaline is a typical accessory mineral in both simple and complex pegmatite bodies (Lahti, 1981).

The Viitaniemi pegmatite contains approximately seventy mineral species and is particularly rich in Li, Be and Fe-Mn phosphates (Lahti, 1989). The pegmatite body (c. 100 x 10 x >200 m), which was mined for feldspar during 1935–1965, cuts the mica schist (Lahti, 1989). Black tourmalines (T1) are common in the distal parts of the pegmatite body and represent an early magmatic phase (S. Lahti, pers. comm. 2008). Green tourmalines (T2), which formed during a volatile-rich phase, exist in the inner parts of the body (S. Lahti, pers. comm. 2008).

The subhorizontal Juurakko pegmatite dyke lies near the contact of a granite stock and cuts the mica schist and a minor dioritic intrusion (Lahti, 1989). The pegmatite deposit was found as early as 1916 and was quarried during 1930–1966 (Lahti, 1989). Black tourmaline crystals (T3) are abundant within the zoned pegmatite dyke (Lahti, 1989).

A network of Li-bearing pegmatite lenses and dykes is found in the mica schist next to a granitoid

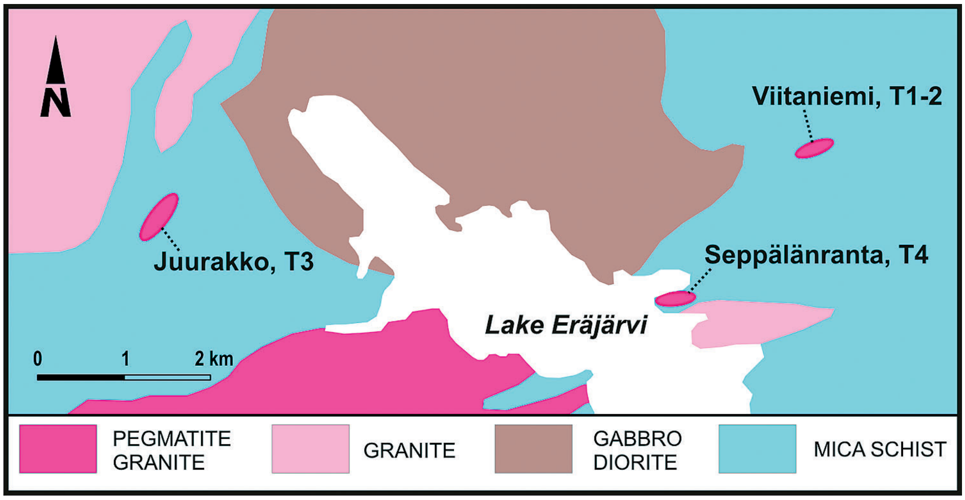

**Fig. 2.** Generalised geological map of the Eräjärvi area (simplified after Lahti, 1989).

in the Seppälänranta area where a small-scale quarry was operated in the 1930s (Lahti, 1989). The pegmatite contains black, green, blue and red tourmalines (Lahti, 1989). The Li-rich red tourmalines (T4) crystallised from late volatile-rich fluids (S. Lahti, pers. comm. 2008).

## 3.2 Sample T5, Riukka gold occurrence, Tammela

The Riukka orogenic gold prospect is located within the Forssa group of the volcano-sedimentary Häme Belt. The geochemical composition of the metavolcanic rocks varies from basaltic andesite to dacite, and they have been metamorphosed under lower amphibolite facies conditions and deformed during the Svecofennian orogeny (Hakkarainen, 1994). The 1890–1880 Ma granodiorites, tonalites and quartz diorites, some of which may represent subvolcanic sills, intruded into the supracrustal sequence (Saalmann, 2007). The closest 1840–1820 Ma, microcline granite is located less than 5 km to the east from the Riukka gold occurrence (Saalmann, 2007).

The gold mineralisation is controlled by shear zones that cut the intermediate and mafic metavolcanic rocks and a felsic dyke (Kärkkäinen et al., 2007). The metavolcanic rocks are altered (biotitisation, chloritisation, silicification, sulphidisation, tourmalinisation) in the vicinity of the shear zones (Kärkkäinen et al., 2007). During the exploration activities by the Geological Survey of Finland, a number of narrow, high-grade zones (up to 35.5 g/t Au over 1 m) in diamond drill core were encountered, but the economic potential of the deposit is yet to be demonstrated (Kärkkäinen et al., 2007).

Gold is mainly related to quartz-tourmaline veins (Fig. 3). Remobilisation of the quartz veins, their formation under divergent stress fields, and periodic growth of gold-bearing mineral grains are evidence for multiple mineralising fluid pulses postdating the peak metamorphism (Etelämäki, 2007; Kärkkäinen et al., 2007; Saalmann, 2007). Recent age data and structural interpretation imply that the mineralising event or remobilisation of an earlier mineralisation occurred at 1830–1800 Ma, and may be linked to the late Svecofennian granitic magmatism (Saalmann et al., 2008). The abundant occurrence of tourmaline as clusters, bands and mass in the metavolcanic rocks and in the quartz veins indicate pervasive hydrothermal fluid activity (Kärkkäinen et al., 2007). Sample T5 comprises fine-grained, dark tourmaline mass from a quartz-tourmaline vein. Arsenopyrite grains are abundant within the tourmaline mass.

## 3.3 Sample T6, Kietyönmäki pegmatite, Tammela

Over one hundred granite-pegmatite or pegmatite lenses, veins and bodies, many of which contain rare

**Fig. 3.** Quartz-tourmaline vein at the Riukka gold occurrence. The diameter of the compass wheel is 6 cm.

earth minerals, are located in the Somero-Tammela region (Alviola, 1989). The Kietyönmäki pegmatite dyke swarm is located c. 500 m to the south-southwest from the Riukka gold occurrence in the contact between mica schist and amphibolite (Virkkunen, 1962; Alviola, 1993). The largest of the Li-bearing subvertical dykes is about 10 m wide and 200 m long. The pegmatite contains black tourmaline crystals (T6) that are 1–1.5 cm in diameter. The formation of the post-tectonic pegmatites is commonly associated with the 1850–1800 Ma late-orogenic granitoids (Alviola, 1989).

## 3.4 Samples T7–8, Kutemajärvi gold deposit, Orivesi

The hydrothermally altered domain, which hosts the metamorphosed epithermal Kutemajärvi gold deposit, is situated on the northern flank of the Tampere Belt and is in contact with the subvolcanic Pukala porphyric intrusion. The altered domain is composed of an outer rim of chlorite-sericite schist and a central part characterised by sericite-quartz schist and andalusite, quartz and topaz rocks (Grönholm, 1992; Luukkonen, 1994). The subvertical, pipe-shaped ore bodies have been mined by Outokumpu Oyj in 1994–2003 and Polar Mining Oy from 2007 onwards. By the end of 2010, the mine had produced 510 000 ounces of gold.

A zircon U-Pb age of 1904±4 Ma was obtained for the unaltered metavolcanic rock (Koskuenjärvi formation) of the Tampere Belt, located in the vicinity of the Kutemajärvi area (Kähkönen et al., 1989). The Pukala intrusion has a zircon U-Pb age of 1896±4 Ma and a titanite age of 1851±4.6 Ma (Talikka & Mänttäri, 2005). The pervasive alteration at Kutemajärvi is linked to the emplacement of the Pukala intrusion and precedes the main regional metamorphism and deformation (Talikka, 2007). Samples T7 and T8 are from quartz-tourmaline veins that cut the hydrothermally altered rocks at the Orivesi gold mine. The formation of the quartz-tourmaline veins postdates the main hydrothermal alteration, deformation and gold mineralisation event.

Sample T7 is fine-grained, schistose, dark tourmaline and forms ragged but continuous sections in a quartz-tourmaline vein. Pyrite and chalcopyrite grains exist in the contacts between quartz and tourmaline.

Sample T8 is fine-grained, slightly foliated and in places massive tourmaline from a quartz-tourmaline vein. The tourmaline-rich section is c. 2 cm wide and has an irregular shape. A few small pyrite grains exist in the sample.

## 3.5 Sample T9, Lepomäki gold occurrence, Hämeenkyrö

The Lepomäki gold occurrence is located in the western part of the volcano-sedimentary Tampere Belt, 4 km to the north of the Ylöjärvi Cu-W-As-Ag-Au deposit. The elevated gold concentrations are related to a set of subvertical tourmaline±quartz veins that cut rhyolitic, dacitic and andesitic metavolcanic rocks at the contact between the synorogenic Hämeenkyrö batholith and the supracustal rocks of the Tampere Belt (Lehto & Vuori, 2006). The veins are typically less than 50 cm wide and some of them exhibit a breccia texture. The high gold grades (up to 55 g/t Au) in arsenopyrite-bearing tourmaline-quartz vein samples found by amateur prospectors could not be reproduced by the Geological Survey of Finland in 2000–2004. Exploration activities identified elevated but subeconomic gold values, yielding less than 0.3 g/t Au (Lehto & Vuori, 2006). According to Lehto and Vuori (2004), the mineralisation at Lepomäki may be associated with the formation of the tourmaline-breccia hosted Cu-W-As-Ag-Au Ylöjärvi deposit and the emplacement of the Hämeenkyrö batholith. Sample T9 is from a quartz-tourmaline vein and contains dark, fine-grained tourmaline crystals and foliated tourmaline mass.

## 3.6 Sample T10, Ylöjärvi Cu-W-Ag-As-Au deposit, Ylöjärvi

The Ylöjärvi Cu-W-Ag-As-Au deposit is situated in the western part of the Tampere Belt in the metavolcanic rocks immediately to the east from the synorogenic Hämeenkyrö batholith (Himmi et al., 1979). The deposit was mined during 1942–1966 and produced 28 322 tonnes of copper, 49.5 t of silver, 0.27 t of gold, 427 t of tungsten and 567 t of arsenic from c. 4 Mt of ore (Himmi et al., 1979). The ore deposit is hosted by one of the several tourmaline breccia (T10) bodies that extend from the Hämeenkyrö batholith into the country rocks (Himmi et al., 1979; Nironen, 1989b). In addition to tuffitic fragments, the tourmaline breccia contains chalcopyrite, arsenopyrite, pyrrhotite, scheelite and other accessory minerals (Himmi et al., 1979). A zircon U-Pb age for the Hämeenkyrö batholith is 1885±2 Ma and uraninite from the tourmaline breccia has a $^{207}Pb/^{206}Pb$ age of 1890 Ma (Himmi et al., 1979; Nironen, 1989a). It has been suggested that the ore-bearing tourmaline breccia bodies that cut the metavolcanic rocks formed after regional metamorphism and deformation and that the Hämeenkyrö batholith was the source for the ore-forming fluids (Himmi et al., 1979).

## 4. Sample preparation and analytical methods

The analysed tourmaline grains (crushed tourmaline crystals or fine-grained tourmaline mass) were handpicked to minimize the risk of contamination, particularly in the fine-grained tourmaline samples that typically contain accessory minerals. The same tourmaline grains (typically two spots per grain) were used for EPMA and SIMS analysis, and at least four different grains were investigated for major element composition and two grains for boron isotopic composition from each sample (Fig. 4). Potential zoning within the tourmaline crystals and grains was not investigated. Marschall and Ludwig (2006), and Smith and Yardley (1996) indicate that isotopic zonation of B is rare despite well-developed chemical zonation.

The major element compositions were determined using a Cameca SX100 electron microprobe analyzer (EPMA) at the Geological Survey of Finland. The used acceleration voltage was 15 kV and electron probe current 20nA. The beam diameter was defocused to 5 μm. Well-characterized natural minerals were used as reference standards for the quantitative analyses. The following x-ray lines and reference standards were used: Si Kα, Ca Kα and Mg Kα from diopside, Al Kα and Fe Kα from almandine, Mn Kα from rhodonite, Ti Kα from rutile, K Kα from sanidine, F Kα from fluorite and Na Kα from tugtupite. The matrix correction calculations were made using PAP correction procedures introduced by Pouchou and Pichoir (1985). $B_2O_3$ concentrations were calculated to 3 B per formula unit, $H_2O$ contents to 4 (H + F + Cl) per formula unit, and structural formulae on the basis of 24.5 oxygens using WinClastour software by Yavuz et al. (2006).

The B isotopic values were measured using a Cameca ims 1270 multicollector secondary ionization mass spectrometer (SIMS) at the University of Edinburgh. Positive secondary ions of $^{10}B+$ and $^{11}B+$ were produced by a 8 nA, 22 keV, $^{16}O_2$- primary beam focused to a ~25 μm spot size. The secondary ions were analysed with a mass resolution of ~ 2000

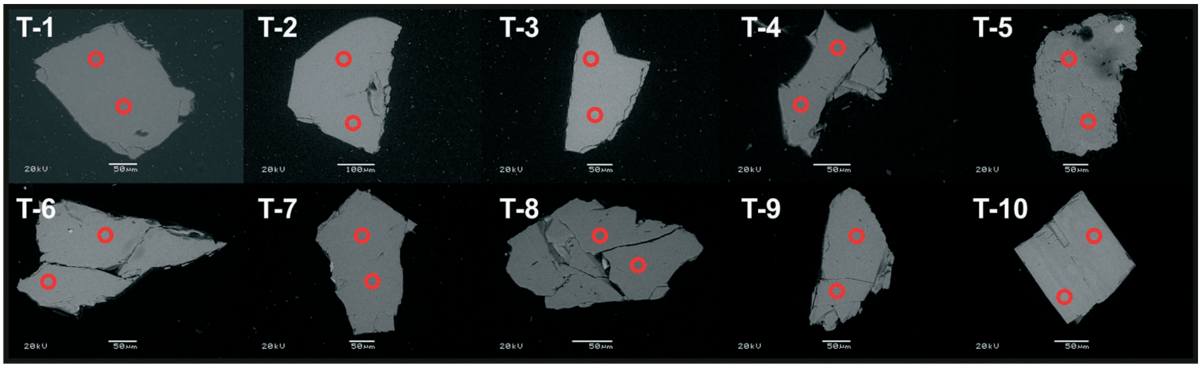

**Fig. 4.** Examples of the analysed tourmaline samples and targeted spots.

(sufficient to resolve mass interferences of $^{9}Be^{1}H+$ (M=1400) and $^{10}B^{1}H+$ ( M=900)) using an energy window of 50 eV, a 150 µm image field, a 400 µm contrast and a 6000 µm field aperture. The B isotope ratios were measured for 20 cycles, each cycle consisting of 5 and 2 second count times on $^{10}B+$ (~1 x $10^7$ cps) and $^{11}B+$ respectively, using Faraday cup in single collector mode operation. Prior to each analysis, the samples were presputtered for 2 minutes to remove surface contamination. Data are reported in the conventional $\delta$ per mil (‰) notation relative to NIST SRM 951 (Catanzaro et al., 1970). Calibration to reference material was through tourmaline 112566 (schorl) using the recommended $\delta^{11}B$ value of -12.5± 0.05 ‰ ($1\sigma$) from Dyar et al. (2001) and Leeman and Tonarini (2001). Additional measurements were made on reference tourmaline elbaite 98144 (-10.5 ± 0.2 ‰) (Dyar et al., 2001; Leeman & Tonarini, 2001). The internal precisions ($1\sigma_{mean}$) for analysis range between 0.3 and 1.0 ‰ (Table 1).

# 5. Results

## 5.1 Tourmaline chemistry

The chemical composition (Table 1) of the tourmaline samples exhibit distinct variations reflecting the environment of formation. The host rock lithologies of the samples correlate well with the predefined fields in the Al-Fe-Mg and Ca-Fe-Mg plots (Figs. 5 & 6) of Henry and Guidotti (1985). Samples (T1–4, T6) from the Eräjärvi and Kietyönmäki granite pegmatites fall into the fields of Li-rich or Li-poor granitoids and associated rocks, and the tourmaline vein samples (T5, T7–8) from the Riukka and Kutemajärvi gold occurrences fit into the field that represents supracrustal rocks (Henry & Guidotti, 1985). On the basis of the Al-Fe-Mg plot, sample (T10) from the tourmaline-breccia hosted Ylöjärvi polymetallic deposit displays the characteristics of $Fe^{3+}$-rich quartz-tourmaline rocks and hydrothermally altered granites (Henry & Guidotti, 1985). The tourmaline vein/breccia sample (T9) from Lepomäki plots into the border region of the fields for granitoid-related and supracrustal rocks (Fig. 5).

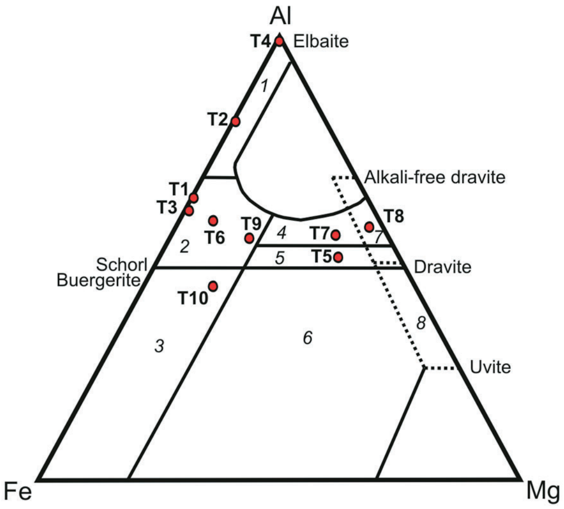

**Fig. 5.** Geochemical compositions of the tourmaline samples (T1–10) in Al-Fe(tot)-Mg diagram. Fields for different rock types after Henry and Guidotti (1985). (1) Li-rich granitoid pegmatites and aplites, (2) Li-poor granitoids and their associated pegmatites and aplites, (3) $Fe^{3+}$-rich quartz-tourmaline rocks (hydrothermally altered granites), (4) Metapelites and metapsammites coexisting with an Al-saturating phase, (5) Metapelites and metapsammites not coexisting with an Al-saturating phase, (6) $Fe^{3+}$-rich quartz-tourmaline rocks, calc-silicate rocks and metapelites, (7) Low-Ca metaultramafic rocks and Cr-, V-rich metasedimentary rocks, and (8) Metacarbonates and metapyroxenites.

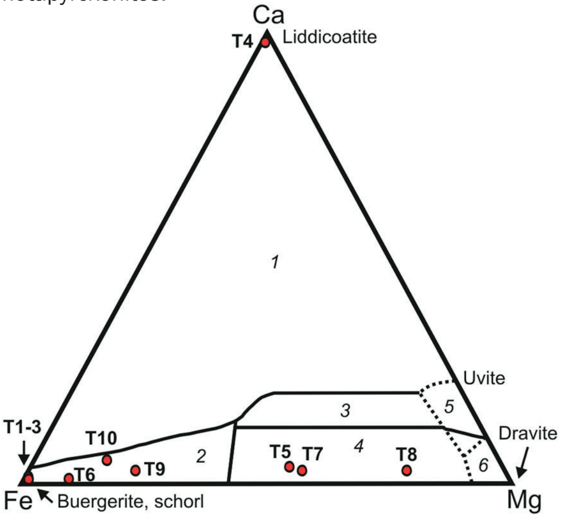

**Fig. 6.** Geochemical compositions of the tourmaline samples (T1–10) in Ca-Fe(tot)-Mg diagram. Fields for different rock types after Henry and Guidotti (1985). (1) Li-rich granitoid pegmatites and aplites, (2) Li-poor granitoids and their associated pegmatites and aplites, (3) Ca-rich metapelites, metapsammites and calc-silicate rocks, (4) Ca-poor metapelites, metapsammites and quartz-tourmaline rocks, (5) Metacarbonates, (6) Metaultramafics.

**Table 1.** Geochemical and boron isotopic compositions of the tourmaline samples.

| Sample<br>Host rock<br>Species | T1<br>GRPG<br>Schorl | T2<br>GRPG<br>F-Schorl | T3<br>GRPG<br>F-Schorl | T4<br>GRPG<br>F-Elbaite | T5<br>VEIN<br>Dravite | T6<br>GRPG<br>Schorl | T7<br>VEIN<br>Dravite | T8<br>VEIN<br>F-Dravite | T9<br>VEIN<br>Schorl | T10<br>TURMBR<br>Oxy-Schorl |
|---|---|---|---|---|---|---|---|---|---|---|
| Electron microprobe - Geochemical analysis, average compositions | | | | | | | | | | |
| n= | 15 | 8 | 8 | 8 | 7 | 8 | 12 | 10 | 9 | 12 |
| $SiO_2$ | 34.36 | 36.08 | 34.15 | 37.17 | 36.24 | 34.40 | 36.45 | 37.36 | 35.40 | 34.22 |
| $TiO_2$ | 0.23 | 0.05 | 0.23 | 0.00 | 0.28 | 0.33 | 0.21 | 0.04 | 0.19 | 0.22 |
| $B_2O_3$* | 10.14 | 10.37 | 10.07 | 10.67 | 10.48 | 10.11 | 10.61 | 10.90 | 10.27 | 9.84 |
| $Al_2O_3$ | 33.96 | 36.63 | 33.12 | 40.82 | 30.61 | 32.38 | 33.01 | 34.80 | 31.66 | 26.39 |
| $FeO_t$ | 13.40 | 5.83 | 14.61 | 0.01 | 5.38 | 13.51 | 4.45 | 1.08 | 11.67 | 17.72 |
| MnO | 0.72 | 1.42 | 0.31 | 1.37 | 0.03 | 0.34 | 0.05 | 0.01 | 0.01 | 0.05 |
| MgO | 0.08 | 0.03 | 0.16 | 0.00 | 8.81 | 1.55 | 8.03 | 9.57 | 3.77 | 3.44 |
| CaO | 0.08 | 0.07 | 0.08 | 0.77 | 0.58 | 0.11 | 0.38 | 0.40 | 0.38 | 1.00 |
| $Na_2O$ | 1.78 | 3.01 | 1.94 | 1.90 | 2.48 | 2.01 | 1.95 | 1.77 | 1.96 | 2.27 |
| $K_2O$ | 0.03 | 0.03 | 0.04 | 0.01 | 0.01 | 0.04 | 0.01 | 0.01 | 0.02 | 0.03 |
| F | 0.38 | 1.93 | 0.84 | 1.53 | 0.15 | 0.36 | 0.28 | 0.95 | 0.19 | 0.15 |
| Total | 95.16 | 95.45 | 95.55 | 94.25 | 95.06 | 95.14 | 95.44 | 96.90 | 95.53 | 95.33 |
| $H_2O$** | 3.315 | 2.663 | 3.077 | 2.954 | 3.548 | 3.317 | 3.527 | 3.312 | 3.454 | 3.324 |
| Cl | 0.001 | 0.002 | 0.003 | 0.003 | 0.003 | 0.002 | 0.003 | 0.002 | 0.002 | 0.006 |
| =O-F | 0.162 | 0.811 | 0.352 | 0.645 | 0.061 | 0.152 | 0.120 | 0.399 | 0.080 | 0.062 |
| Total | 98.64 | 98.92 | 98.98 | 97.85 | 98.68 | 98.61 | 99.09 | 100.61 | 99.06 | 98.72 |
| Structural formula on the basis of 24.5 oxygens | | | | | | | | | | |
| B | 3.000 | 3.000 | 3.000 | 3.000 | 3.000 | 3.000 | 3.000 | 3.000 | 3.000 | 3.000 |
| Si | 5.891 | 6.048 | 5.895 | 6.056 | 6.007 | 5.912 | 5.967 | 5.957 | 5.989 | 6.043 |
| Ti | 0.030 | 0.006 | 0.030 | 0.000 | 0.035 | 0.043 | 0.026 | 0.005 | 0.024 | 0.029 |
| Al | 6.863 | 7.238 | 6.737 | 7.838 | 5.980 | 6.559 | 6.369 | 6.538 | 6.311 | 5.493 |
| Fe | 1.921 | 0.818 | 2.110 | 0.001 | 0.746 | 1.941 | 0.610 | 0.144 | 1.652 | 2.617 |
| Mn | 0.104 | 0.202 | 0.045 | 0.189 | 0.004 | 0.050 | 0.007 | 0.002 | 0.002 | 0.008 |
| Mg | 0.020 | 0.008 | 0.040 | 0.000 | 2.178 | 0.397 | 1.959 | 2.276 | 0.951 | 0.906 |
| Ca | 0.015 | 0.013 | 0.015 | 0.135 | 0.103 | 0.020 | 0.067 | 0.068 | 0.069 | 0.190 |
| Na | 0.592 | 0.977 | 0.651 | 0.600 | 0.798 | 0.671 | 0.621 | 0.547 | 0.644 | 0.776 |
| K | 0.006 | 0.005 | 0.008 | 0.002 | 0.003 | 0.009 | 0.002 | 0.002 | 0.003 | 0.006 |
| F | 0.208 | 1.022 | 0.456 | 0.789 | 0.077 | 0.197 | 0.147 | 0.477 | 0.102 | 0.083 |
| Fe/(Fe+Mg) | 0.990 | 0.990 | 0.981 | 1.000 | 0.255 | 0.830 | 0.237 | 0.060 | 0.635 | 0.743 |
| Fe+Mg | 1.941 | 0.826 | 2.150 | 0.001 | 2.924 | 2.338 | 2.569 | 2.419 | 2.602 | 3.523 |
| Secondary ionization mass spectrometer - Boron isotopic composition - $\delta^{11}$B (‰), $1\sigma_{mean}$ (‰) | | | | | | | | | | |
| #1, $\delta^{11}$B ($1\sigma$) | -10.7 (1.0) | -13.7 (1.0) | -10.6 (0.5) | -9.2 (0.5) | -9.4 (1.0) | -13.5 (0.6) | -11.2 (0.6) | -10.5 (0.6) | -9.3 (0.6) | -7.8 (0.5) |
| #2, $\delta^{11}$B ($1\sigma$) | -12.1 (0.5) | -11.6 (0.6) | -10.5 (0.3) | -11.7 (0.5) | -10.8 (1.0) | -12.8 (0.5) | -10.7 (0.6) | -9.9 (0.9) | -9.2 (0.8) | -7.8 (0.3) |
| #3, $\delta^{11}$B ($1\sigma$) | -12.6 (0.8) | -13.4 (0.9) | -10.6 (0.7) | -11.7 (0.5) | -12.5 (0.8) | -12.1 (0.5) | -11.8 (0.8) | | | -9.8 (0.5) |
| #4, $\delta^{11}$B ($1\sigma$) | -11.2 (0.8) | -14.1 (0.9) | -9.8 (0.5) | | -13.5 (0.6) | | | | | -9.4 (0.5) |
| #5, $\delta^{11}$B ($1\sigma$) | | | -9.5 (0.7) | | | | | | | |
| $\delta^{11}$B mean | -11.7 | -13.2 | -10.2 | -10.9 | -11.6 | -12.8 | -11.2 | -10.2 | -9.3 | -8.7 |

Secondary ionization mass spectrometer - Boron isotopic composition, Reference tourmalines - $\delta^{11}$B (‰),$1\sigma_{mean}$ (‰)

Elbaite 98144 (-10.5 ± 0.2‰): -10.5 (1.0), -9.2 (1.0), -9.6 (0.5), -10.4 (0.5), -9.0 (0.8), -11.1 (0.8), -11.9 (0.7), -11.8 (0.7), -10.6 (0.7), -10.8 (0.8), -9.7 (0.8), -9.3 (0.8), -10.2 (0.8), -9.9 (0.8).

Schorl 112566 (-12.5 ± 0.05‰): -12.6 (0.6), -12.5 (0.4), -12.5 (0.5), -12.5 (0.6), -12.4 (0.4), -13.0 (0.4), -12.3 (0.3), -12.2 (0.3), -12.9 (0.8), -12.1 (0.4).

*$B_2O_3$ contents calculated stoichiometrically to 3 B per formula unit.

**$H_2O$ contents calculated stoichiometrically to 4 (H+F+Cl) per formula unit.

Structural formulae and species determinations by using Winclastour software (Yavuz et al. 2006).

Abbreviations: GRPG = granite pegmatite, TURMBR = tourmaline breccia.

The red tourmaline sample (T4) from the Seppälänranta quarry differs from other samples from the Eräjärvi pegmatite cluster by having higher CaO and $Al_2O_3$, and lower MgO and FeO contents (Fig. 6). Samples (T1–2) from the Viitaniemi quarry show distinct differences in their geochemical compositions, for instance, in $Na_2O$ and FeO contents. Of the granite pegmatite hosted tourmalines, the Kietyönmäki sample (T6) has by far the highest MgO content. The vein-related tourmaline samples (T7–8) from the Kutemajärvi differ from each other by concentrations of MgO and $TiO_2$. Samples (T9–10) from Lepomäki and Ylöjärvi show notable variations, for instance, in their FeO and $Al_2O_3$ contents.

Pirajno and Smithies (1992) suggested that the FeOt/(FeOt+MgO) ratio of tourmalines reflects the distance from a granitic source. The Fe/(Fe+Mg) ratio of the studied samples varies between 0.06 and 1.00. In the FeOt/(FeOt+MgO) vs. MgO plot (Fig. 7), samples from the granite pegmatites, veins, and contact region between intrusion and supracrustal rocks represent their expected environment of formation (Pirajno & Smithies, 1992).

## *5.2 Boron isotopic composition*

The results for each B isotopic analysis and mean values are presented in Table 1. Due to the limited amount of the B isotopic data, the results and interpretations should be regarded as indicative. The mean $\delta^{11}B$ values of the tourmaline samples range from -13.2 ‰ to -8.7 ‰. The $\delta^{11}B$ values of tourmalines (T1-4, T6) from the granite pegmatites (-10.2 ‰ – -13.2 ‰) are comparable with the vein-related (T5, 7-8) tourmalines (-10.2 ‰ – -11.6 ‰). The intrusion-country rock contact-related tourmalines (T9–10) have lighter B isotopic composition (-9.6 ‰, -8.7 ‰).

The B isotopic compositions of the studied samples are in accordance with previous studies worldwide (Fig. 8) (Jiang & Palmer, 1998). In their synthesis paper Jiang and Palmer (1998) showed that the B isotopic data of granitic and pegmatitic tourmalines clusters between -15 ‰ and -5 ‰ (total range -30 ‰ – +8 ‰), and that, in the local scale, tourmalines from granite-related veins generally have greater $\delta^{11}B$ values compared to tourmalines within granite bodies.

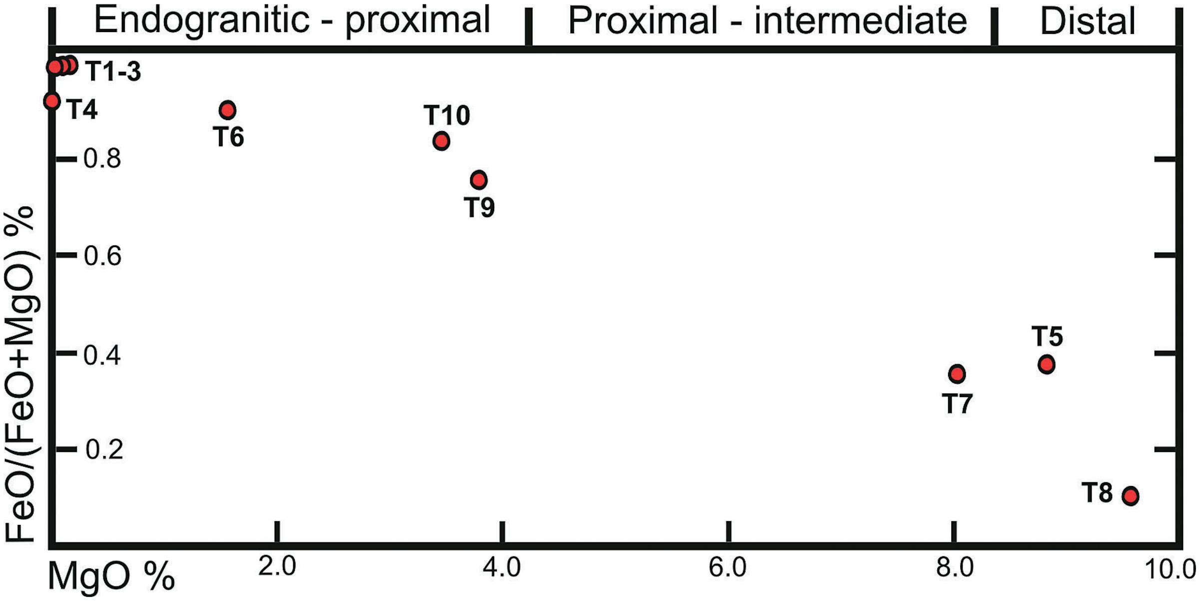

**Fig. 7.** Geochemical compositions of the tourmaline samples (T1–10) in FeO/(FeO+MgO) vs. MgO plot. After Pirajno and Smithies (1992) and Yavuz et al. (2006).

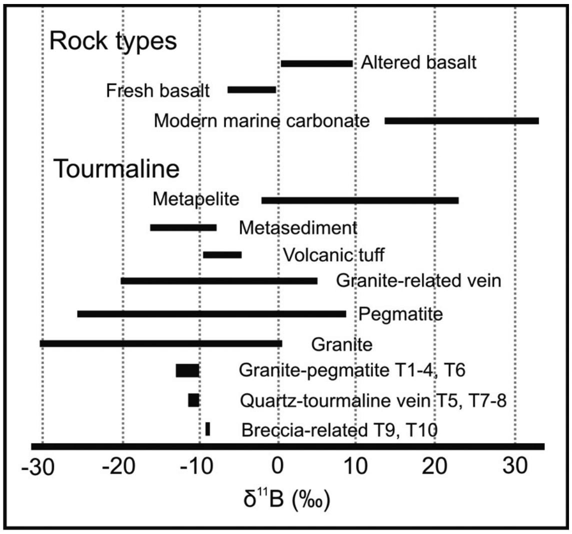

**Fig. 8.** $\delta^{11}B$ values of the tourmaline samples (T1-10) compared to the $\delta^{11}B$ values of rock types and tourmalines from various host lithologies. Modified from Jiang and Palmer (1998).

# 6. Discussion

## 6.1 Boron and tourmaline

The high geochemical reactivity of B and the vast relative mass difference between isotopes ($^{10}B$ and $^{11}B$) lead to significant isotopic fractionation by natural processes (Barth, 1993). In igneous systems, B is an incompatible element and concentrated in residual melts during crystal fractionation, resulting in enrichment of B in felsic and silicic melts (London et al., 1996). The presence of B also affects the genesis of melts by lowering the liquidus and solidus temperatures, and by increasing the solubility of $H_2O$ in melt (Holz et al., 1993; Dingwell et al., 1996; London et al., 1996; Jiang & Palmer, 1998). Because tourmaline is the dominant B-bearing mineral in most geologic settings, the $\delta^{11}B$ value does not change during recrystallisation of tourmaline in a closed system during metamorphism (Palmer & Swihart, 1996). In an open system, $^{11}B$ is enriched into the fluid phase leaving the recrystallised tourmaline enriched in $^{10}B$ (Palmer et al., 1992). The B isotopic composition of granite and granite-related vein hosted tourmalines is mainly established by pressure-temperature conditions, magma degassing, the composition of the magma source and interaction with the country rocks (Jiang & Palmer, 1998). Ranges for typical $\delta^{11}B$ values for rock types, tourmalines from various lithologies and tourmalines from this study are presented in Figure 8.

One of the primary processes that may lead to the B isotopic fractionation in the formation of plutonic rocks is magmatic degassing (Jiang & Palmer, 1998). Experimental studies show that the B isotopic fractionation between silica melt and vapour is greater than between tourmaline and vapour at 650–750 °C and 200 Mpa (Palmer et al., 1992; Hervig et al., 1997). Boron forms tetrahedral $[B(OH)_{4-}]$ complexes in the melt and trigonal $[B(OH)_{3-}]$ complexes in the aqueous fluids, and only the trigonal B species is stable under the pH range (< 6.5) of tourmaline (Pichavant, 1983; Hershey et al., 1986; Morgan & London, 1989; Chakraborty et al., 1993). This is the likely reason for the large B fractionation during magmatic degassing that leads to the depletion of $^{11}B$ in the melt (Kotaka, 1973; Kakihana et al., 1977; Jiang & Palmer, 1998). As a result, tourmalines in hydrothermal veins generally have higher $\delta^{11}B$ values than magmatic tourmalines in the same system (Jiang & Palmer, 1998). If tourmaline crystallises from melt that has not been affected by the B isotopic fractionation, the $\delta^{11}B$ values of the melt and tourmalines are similar (Jiang & Palmer, 1998). Studies suggest that fine-grained tourmalines may crystallise from a granitic melt before the B isotopic fractionation and that large magmatic tourmalines crystallise from late, evolved fluids (London & Manning, 1995; Jiang & Palmer, 1998). Magmatic tourmalines within a single intrusion, however, may also show variations in their $\delta^{11}B$ values, for example, if magmatic degassing occurred during or between the crystallisation events or a new magma pulse with different properties was introduced into the system.

The formation of tourmaline requires enriched B concentration in the melt or fluid and a flux of other elements such as Fe and Mg that are typically derived from the adjacent country rocks. The major element compositions of the studied tourmalines reflect their geologic setting and are in accordance with the results of previous studies. Intrusion-related and vein-related samples can be classified by their Fe, Mg, Ca and Al contents as demonstrated in figures 5 and 6 (Henry & Guidotti, 1985). In terms of their FeO/(FeO+MgO) ratios, the tourmaline samples form three groups (Fig. 7) that correlate with the presumed distance from a granitic source during their formation (Pirajno & Smithies, 1992). On the basis of their mode of occurrence, the tourmaline samples can be divided into three groups: granite pegmatite-related (T1–4, T6), vein-related (T5, T7–8) and intrusion-country rock contact-related (T9–10).

## 6.2 Granite pegmatite-related tourmalines

Granite pegmatite-related tourmalines show distinct variations, for instance, in their Fe, Mg, Na, Ca and F contents. Black (schorl) tourmalines (T1, T3) from the Eräjärvi pegmatites show characteristics of Li-poor granitoids, and green (T2) and red (T4) tourmalines the characteristics of Li-rich granitoids (Fig. 5), despite that all host lithologies contain Li-bearing minerals (Lahti, 1989). In addition, the divergent samples T1 and T2 are from the same Viitaniemi pegmatite dyke. The black (schorl) tourmalines (T1) may have formed during the early magmatic phase and the green tourmalines (T2) from volatile-rich melt postdating the B isotopic fractionation (S. Lahti, pers. comm. 2008). This is supported by the lower $\delta^{11}$B values of the green tourmaline sample (T2, Table 1). The compositional variations in the melt and fluctuating interaction between the melt, fluids and country rocks provide another possible explanation for the variations in the chemical compositions of tourmalines at Eräjärvi.

All tourmalines (T1–4, T6) from the late-orogenic pegmatites have broadly similar B isotopic signatures (-10.2 ‰ – -13.2 ‰). The relatively constant $\delta^{11}$B values indicate that the material for the pegmatites was derived from a similar source. Sample (T6) from the Kietyönmäki pegmatite has comparable B isotopic composition with the Eräjärvi samples despite some differences in the major element compositions of the tourmalines. The tenfold MgO concentration of sample T6 may reflect the presence of amphibolite among the country rocks at Kietyönmäki compared to the mica schist at Eräjärvi.

## 6.3 Vein-related tourmalines

Vein-related tourmaline samples (T5, T7–8) comprise fine-grained tourmaline mass, and can be distinguished from other samples by their higher MgO contents. $\delta^{11}$B values of the vein-related tourmalines are similar or slightly higher compared to the granite pegmatite-related tourmalines (T1–4, T6). If the vein-related tourmalines are associated with felsic magmatism without a significant contamination from the country rocks, their B isotopic compositions may represent either an unfractionated melt or a fractionated phase enriched in $^{11}$B.

The quartz-tourmaline veins at Kutemajärvi (T7–8) postdate the main hydrothermal alteration, deformation and gold mineralising event and show relatively uniform $\delta^{11}$B values (-10.2 ‰, -11.2 ‰). The quartz-tourmaline vein from the Riukka gold occurrence (T5) shows a wide range in its $\delta^{11}$B values (-9.4 ‰ – -13.5 ‰). The variations may indicate that the formation of tourmalines occurred during several fluid pulses containing different B isotopic compositions. Leaching of previously crystallised tourmaline by later fluid pulses may also result in increasing $\delta^{11}$B values in fluid towards the end of the hydrothermal event. Previous studies suggest that the hydrothermal activity at Riukka postdates the peak metamorphism and was active during several stages (Etelämäki, 2007; Kärkkäinen et al., 2007; Saalmann, 2007). The formation of the granite-migmatite zone of southern Finland at 1830–1810 Ma may have contributed to the hydrothermal activity (Väisänen et al., 2002; Saalmann et al., 2008).

## 6.4 Intrusion-country rock contact-related tourmalines

The fine-grained tourmaline vein/breccia samples from Lepomäki (T9) and Ylöjärvi (T10) represent a contact region between the syn-orogenic Hämeenkyrö batholith and its country rocks. Their chemical composition, for example MgO content (mean 3.6 %), is between those of the granite pegmatite (MgO <1.6 %) and vein (MgO >8.4 %) related tourmalines.

Intrusion-country rock-related tourmalines show lighter B isotopic composition (-9.6 ‰ – -8.7 ‰) than the granite pegmatite-related tourmalines (-10.2 ‰ – -13.2 ‰), which could be an evidence for divergent B reservoirs and a mode of formation between the syn- and late-orogenic tourmalines.

### *6.5 Tourmaline: A link to hydrothermal systems and mineralising events?*

During an orogenic cycle, supracrustal rocks containing minor B are subjected to increasing pressure and temperature conditions, and enrichment of B via geochemical processes may lead to the formation of magmatic or hydrothermal systems with elevated B content. In igneous rocks, B is an incompatible element and has a significant impact on the magmatic and hydrothermal processes. Some ore deposit types, for example, orogenic gold style mineralisations, form as a result of enrichment of metals by hydrothermal circulation. Even if B was not directly linked to the ore mineralising event, it may have contributed to the evolution of the associated hydrothermal system.

At the Riukka and Lepomäki gold and Ylöjärvi polymetallic occurrences, tourmaline is associated with the ore minerals (Himmi et al., 1979; Lehto & Vuori, 2004; Kärkkäinen et al., 2007). At these localities, B and ore minerals may share a common origin. A likely source for the fluids and metals at Lepomäki and Ylöjärvi is the adjacent Hämeenkyrö batholith (Himmi et al., 1979). The source for the mineralising fluids at Riukka remains unclear.

## 7. Conclusions

The formation of tourmaline is a highly complex process and controlled by a number of factors such as the fluid and host rock chemistry, activity of $H_2O$ and P-T conditions. The widespread existence and the protean nature of tourmaline, however, provide useful information on various geological processes. As demonstrated here and in previous studies (e.g. Henry & Guidotti, 1985; Palmer & Slack, 1989), the major element composition of tourmalines is controlled by their host lithologies. Granite pegmatite, vein and granitoid-country rock contact-related tourmalines can be distinguished by their major element compositions.

On the contrary, the B isotopic composition of tourmalines typically does not have an evident correlation with the major element composition. The mean $\delta^{11}B$ values of the investigated tourmalines range from -13.2 ‰ to -8.7 ‰ and are in accordance with other terrestrial samples (e.g. Jiang & Palmer, 1998). Tourmalines from the late-orogenic granite pegmatites at Eräjärvi and Kietyönmäki have fairly uniform B isotopic compositions (-10.2 ‰ – -13.2 ‰) that are comparable with the $\delta^{11}B$ values of the vein-related tourmalines (-10.2 ‰ – -11.6 ‰). Tourmalines linked to the formation of the synorogenic Hämeenkyrö batholith have distinctly lighter B isotopic composition (-9.6 ‰ – -8.7 ‰) indicating a difference in the B reservoirs and formational processes between the syn- and late-orogenic tourmalines.

Field observations and geochemical data indicate that the formation of tourmaline was intimately associated with the gold mineralising events at Lepomäki, Riukka and Ylöjärvi. The B isotopic and geochemical data from Ylöjärvi and Lepomäki supports the primary role of the Hämeenkyrö batholith as the dynamo and source for the hydrothermal system. At Riukka, the presence of multiple fluid pulses may explain the large variations in the $\delta^{11}B$ values of tourmalines. A possible explanation for the long-lasting hydrothermal circulation is the late Svecofennian granitic magmatism and migmatitisation in southern Finland. The coexistence of tourmaline bearing rocks and gold occurrences in southwestern Finland suggests that the formation of tourmalines and gold mineralising events are in some cases parts of the same magmatic-hydrothermal processes which occurred during the syn- and late-orogenic phases of the Svecofennian orogeny.

As a resistant mineral to weathering and metamorphism, and due to its widespread existence in different lithologies, tourmaline is a suitable object for a number of research topics. The aim of this pilot study is to lay a basis for more detailed studies on tourmalines and their relation to magmatic and hydrothermal systems associated with gold mineralisation processes, and to encourage the development of applications for gold and other metal exploration.

## Acknowledgements

Dr. Simone Kasemann (Univ. of Edinburgh) is thanked for the analysis of the B isotopic compositions, and Dr. Bo Johansson (Geological Survey of Finland) for the geochemical analysis. Contributions from Dr. Pasi Eilu, Dr. Seppo Lahti, Dr. Raimo Lahtinen, Dr. Niilo Kärkkäinen, Mrs. Kirsti Keskisaari, Dr. Petri Peltonen, Dr. Matti Poutiainen and Dr. Kerstin Saalmann are acknowledged. Dr. Arto Luttinen and two anonymous referees are thanked for their comments that led to improvements of the manuscript.

## References

Alviola, R. 1989. The granitic pegmatites of the Somero-Tammela area. Geological Survey of Finland, Guide 26, 16–25.

Alviola, R. 1993. Tutkimustyöselostus Tammelan kunnassa, valtausalueella Kietyönmäki 1, kaiv.rek. N:o 3991/1, suoritetuista teollisuusmineraalitutkimuksista. Geological Survey of Finland, Report M06/2024/-93/1/85, 7 p. (in Finnish)

Alviola, R. 2004. Oriveden Seppälä-Viitaniemi alueen pegmatiittitutkimus vv. 2003–2004. Geological Survey of Finland, Report M19/2141/2004/1/85, 9 p. (in Finnish)

Barth, B. 1993. Boron isotopic variations in nature: a synthesis. Geologische Runsdschau 82, 640–651.

Catanzaro, F.J., Champion, C.E., Garner, E.L., Marinenko, G., Sappenfield, K.M. & Shields, W.R. 1970. Boric acid: isotopic and assay standard reference materials. NBS (US) Special Publication 260, 1–70.

Chakraborty, S., Dingwell, D.B. & Chaussidon, M. 1993. Chemical diffusivity of boron in melts of haplogranitic composition. Geochimica et Cosmochimica Acta 57, 1741–1751.

Chaussidon, M. & Albaréde, F. 1992. Secular boron isotope variations in the continental crust: an ion microprobe study. Earth Planet Science Letter 108, 229–241.

Dingwell, D., Pichavant, M. & Holtz, F. 1996. Experimental studies of boron in granitic melts. In: Grew, E.S. & Anovitz, L.M. (eds.) Boron: mineralogy, petrology and geochemistry. Reviews in Mineralogy 33, 331–379.

Dyar, M.D., Wiedenbeck, M., Robertson, D., Cross, L.R., Delaney, J.S., Ferguson, K., Francis, C.A., Grew, E.S., Guidotti, C.V., Hervig, R.L., Hughes, J.M., Husler, J., Leeman, W., McGuire, A.V., Rhede, D., Rothe, H., Paul, R.L., Richards, I. & Yates, M. 2001. Reference minerals for the microanalysis of light elements. Geostandards Newsletter 25, 441–463.

Etelämäki, T. 2007. Tammelan Riukan Au-mineralisaatio. Unpublished M.Sc. thesis, University of Helsinki, 97 p. (in Finnish)

Grönholm, P. 1992. Oriveden Kutemajärven kultaesiintymän ja sen ympäristön geologia. Unpublished M.Sc. Thesis, University of Helsinki, 115 p. (in Finnish)

Hakkarainen, G. 1994. Geology and geochemistry of the Hämeenlinna-Somero Volcanic Belt, Southwestern Finland: A Paleoproterozoic island arc. In: Nironen, M. & Kähkönen, Y. (eds.) Geochemistry of Proterozoic supracrustal rocks in Finland. Geological Survey of Finland, Special Paper 19, 85–100.

Henry, D.J. & Guidotti, C.V. 1985. Tourmaline as a petrogenetic indicator mineral: an example from the staurolite grade metapelites of N.W. Maine. American Mineralogist 70, 1–15.

Henry, D.J. & Dutrow, B.L. 1992. Tourmaline in a low grade clastic metasedimentary rock: an example of the petrogenetic potential of tourmaline. Contributions to Mineralogy and Petrology 102, 203–218.

Hershey, J.P., Femandez, M., Milne, P.J. & Miller, F.J. 1986. The ionisation of boric acid in Na-Cl, Na-Ca-Cl and Na-Mg-Cl solutions at 25°C. Geochimica et Cosmochimica Acta 50, 143–148.

Hervig, R.L., London, D., Morgan, G.B. & Wolf, M.B. 1997. Large boron isotope fractionation between hydrous vapor and silicate melt at igneous temperatures. 7th Annual V.M. Goldschmidt Conf., Lunar Planetary Inst., Houston, LPI contribution No. 921, p. 93–94.

Himmi, R., Huhma, M. & Häkli, T. 1979. Mineralogy and metal distribution in the copper-tungsten deposit at Ylöjärvi, Southwest Finland. Economic Geology 74, 1183–1197.

Holz, F., Dingwell, D. & Behrens, H. 1993. Effects of F, B2O3 and P2O5 on the solubility of water in haplogranite melts compared to natural silicate melts. Contributions to Mineralogy and Petrology 113, 492–501.

Huhma, H., Claesson, S., Kinny, P.D. & Williams, I.S. 1991. Provenance of early Proterozoic Svecofennian metasediments: U-Pb dating of detrital zircons. Geological Survey of Finland, Special Paper 12, 63–65.

Jiang, S. & Palmer, M. 1998. Boron isotope systematics of tourmaline from granites and pegmatites: a synthesis. European Journal of Mineralogy 10, 1253–1265.

Jiang, S., Palmer, M., Slack, J. & Shaw, D. 1998. Paragenesis and chemistry of multistage tourmaline formation in the Sullivan Pb-Zn-Ag deposits, British Columbia. Economic Geology 93, 47–67.

Kähkönen, Y. 1989. Geochemistry and petrology of the metavolcanic rocks of the early Proterozoic Tampere Schist Belt, southern Finland. Geological Survey of Finland, Bulletin 345, 1–104.

Kähkönen, Y. 1999. Stratigraphy of the central parts of the Paleoproterozoic Tampere Schist Belt, southern Finland: review and revision. Bulletin of the Geological Society of Finland 71, 13–29.

Kähkönen, Y. 2005. Svecofennian supracrustal rocks. In: Lehtinen, M., Nurmi, P. & Rämö, O.T. (eds.) Precambrian Geology of Finland – Key to the Evolution of the Fennoscandia Shield. Elsevier, Amsterdam, pp. 343–406.

Kähkönen, Y., Huhma, H. & Aro, K. 1989. U-Pb zircon ages and Rb-Sr whole rock isotope studies of early Proterozoic volcanic and plutonic rocks near Tampere, southern Finland. Precambrian Research 45, 27–43.

Kähkönen, Y. & Leveinen, J. 1994. Geochemistry of metasedimentary rocks of the Paleoproterozoic Tampere Schist Belt, southern Finland. Geological Survey of Finland, Special Paper 19, 117–136.

Kähkönen, Y., Huhma, H. & Mänttäri, I. 2004. TIMS and SIMS U-Pb zircon ages and Rb-Sr whole rock isotope studies of early Proterozoic volcanic rocks near Tampere, southern Finland. In: Mansfield, J. (ed.) The 26th Nordic Geological Winter Meeting, Abstract Volume. Bulletin of the Geological Society of Finland, Special Issue 1, p. 25.

Kakihana, H., Kotaka, M., Satoh, S., Nomura, M. & Okamoto, M. 1977. Fundamental studies on the ion-exchange separation of boron isotopes. Bulletin of the Chemical Society of Japan 50, 158–163.

Kärkkäinen, N., Koistinen, E. & Jokinen, T. 2007. Tutkimustyöselostus malmitutkimuksista Tammelan kunnan Riukan, kaivosrek.nro 7483/1, ja Pursion, kaivosrek.nro 7482/1, valtauksilla. Geological Survey of Finland, Report M06/2024/2007/10/69, 35 p.

Kilpeläinen, T. 1998. Evolution and 3D modelling of structural and metamorphic patterns of the Palaeoproterozoic crust in the Tampere-Vammala area, southern Finland. Geological Survey of Finland, Bulletin 397, 1–124.

Korsman, K., Koistinen, T., Kohonen, J., Wennerström, M., Ekdahl, E., Honkamo, M., Idman, H. & Pekkala, Y. (eds.) 1997. Bedrock Map of Finland. 1:1 000 000. Geological Survey of Finland, Espoo, Finland.

Kotaka, M. 1973. Chromatographic separation of boron and nitrogen isotopes using pure water as eluent. PhD Dissertation, Tokyo Inst Tech.

Lahti, S.I. 1981. On the granitic pegmatites of the Eräjärvi area in Orivesi, southern Finland. Geological Survey of Finland, Bulletin 314, 1–82.

Lahti, S.I. 1989. The granitoids and pegmatites of the Eräjärvi area. Geological Survey of Finland, Guide 26, 26–36.

Lahtinen, R. 1996. Geochemistry of Palaeoproterozoic supracrustal and plutonic rocks in the Tampere-Hämeenlinna area, southern Finland. Geological Survey of Finland, Bulletin 389, 1–113.

Lahtinen, R., Korja, A. & Nironen, M. 2005. Paleoproterozoic tectonic evolution of the Fennoscandian Shield – a plate tectonic model. In: Lehtinen, M., Nurmi, P., Rämö, O.T. (eds.) Precambrian Geology of Finland – Key to the Evolution of the Fennoscandia Shield. Elsevier, Amsterdam, pp. 483–504.

Laitakari, I. 1986. Orivesi. Geological map of Finland 1:100 000, pre-Quaternary rocks, sheet 2142, Geological Survey of Finland, Espoo, Finland.

Leeman, W.P. & Tonarini, S. 2001. Boron isotopic analysis of proposed borosilicate mineral reference samples. Geostandards Newsletter 25, 399–403.

Lehto, T. & Vuori, S. 2004. Kultatutkimukset Hämeenkyrön Lavajärvellä, Pässärinvuoren ja Lepomäen alueilla vuosina 1997-2003. Geological Survey of Finland, Report M19/2124/2004/1/10, 23 p. (in Finnish)

Lehto, T. & Vuori, S. 2006. Tutkimustyöselostus kultatutkimuksista Hämeenkyrön kunnan Lavajärven alueella, valtausalueilla Pärssärinvuori (kaivorek.nro 7277/1) ja Lepomäki kaivosrek.nro 7276/1). Geological Survey of Finland, Report M19/2124/2006/1/10, 19 p. (in Finnish)

London, D. & Manning, D.A.C. 1995. Chemical variations and significance of tourmaline from Southwest England. Economic Geology 90, 495–519.

London, D., Morgan, G. & Wolf, B. 1996. Boron in granitic rocks and their contact aureoles. In: Grew, E.S. & Anovitz, L.M. (eds.) Boron: mineralogy, petrology and geochemistry. Reviews in Mineralogy 33, 299–330.

Luukkonen, A. 1994. Main geological features, metallogeny and hydrothermal alteration phenomena of certain gold and gold-tin-tungsten prospects in southern Finland. Geological Survey of Finland, Bulletin 377, 1–153.

Marschall, H. & Ludwig, T. 2006. Re-examination of the boron isotopic composition of tourmaline from the Lavicke granite, Czech Republic, by secondary ion mass spectrometry: back to normal. Geochemical Journal 40, 631–638.

Morgan, G. & London, D. 1989. Experinmental reaction of amphibolite with boron-bearing aqueous fluids at 200 Mpa: tourmaline stability and partial melting in mafic rocks. Contributions to Mineralogy and Petrology 102, 281–297.

Mouri, H., Korsman, K. & Huhma, H. 1999. Tectono-metamorphic evolution and timing of the melting processes in the Svecofennian Tonalite-Trondhjemite Migmatite Belt: An example from Luopioinen, Tampere Area, southern Finland. Bulletin of the Geological Society of Finland 71, 31–56.

Nironen, M. 1989a. Emplacement and structural setting of granitoids in the early Proterozoic Tampere and Savo Schist Belts, Finland – implications for contrasting crustal evolution. Geological Survey of Finland, Bulletin 346, 1–83.

Nironen, M. 1989b. The syntectonic granitoids of the Tampere area. Geological Survey of Finland, Guide 26, 37–40.

Nironen, M. 2005. Proterozoic orogenic granitoid rocks. In: Lehtinen, M., Nurmi, P. & Rämö, O.T. (eds.) Precambrian Geology of Finland – Key to the Evolution of the Fennoscandia Shield. Elsevier, Amsterdam, pp. 443–480.

Ojakangas, R.W. 1986. An Early Proterozoic metagaywacke-slate turbidite sequence: The Tampere schist belt, southwestern Finland. Bulletin of the Geological Society of Finland 58, 241–261.

Palmer, M.R. 1992. Boron isotope systematics of hydrothermal fluids and tourmalines: A synthesis. Chemical Geology 94, 111–121.

Palmer, M., London, D., Morgan, G. & Babb, H. 1992. Experimental determination of fractionation of 11B/10B between tourmaline and aqueous vapour: A temperature- and pressure-dependent isotopic system. Chemical Geology 101, 123–129.

Palmer, M.R. & Slack, J.F. 1989. Boron isotopic composition of tourmaline from massive sulphide deposits and tourmalinites. Contributions to Mineralogy and Petrology 103, 434–451.

Palmer, M. & Swihart, G. 1996. Boron isotope geochemistry: An overview. In: Grew ES, Anovitz LM (eds.) Boron: mineralogy, petrology and geochemistry. Reviews in Mineralogy 33, 709–744.

Pichavant, M. 1983. Melt-fluid interaction deduced from studies of silicate-B2O3-H2O systems at 1 kbar. Bulletin de Minéralogie 106, 201–211.

Pirajno, F. 1992. Hydrothermal mineral deposits. Springer-Verlag, Berlin, 709 p.

Pirajno, F. & Smithies, R.H. 1992. The FeO/(FeO + MgO) ratio of tourmaline: a useful indicator of spatial variations in granite-related hydrothermal mineral deposits. Journal of Geochemical Exploration 42, 371–381.

Pouchou, J.L. & Pichoir, F. 1985. "PAP" procedure for improved quantitative microanalysis. In: Armstrong, J.T. (ed.) Microbeam Analysis, pp. 104–106.

Saalmann, K. 2007. Structural control on gold mineralization in the Satulinmäki and Riukka prospects, Häme schist belt, southern Finland. Bulletin of the Geological Society of Finland 79, 69–93.

Saalmann, K., Mänttäri, I., Peltonen, P. & Whitehouse, M. 2008. Timing of orogenic gold mineralization in southern Finland and its relationship to the Palaeoproterozoic Svecofennian tectonic evolution. 33rd Internat. Geol. Congress, 6.-14. August, 2008, Oslo, abstract-CD-ROM

Slack, J. 1996. Tourmaline associations with hydrothermal ore deposits. In: Grew, E.S., Anovitz, L.M. (eds) Boron: mineralogy, petrology and geochemistry. Reviews in Mineralogy 33, 559–644.

Smith, M. & Yardley, W. 1996. The boron isotopic composition of tourmaline as guide to fluid processes in the southwestern England orefield: An ion microprobe study. Geochimica et Cosmochimica Acta 60, 1415–1427.

Talikka, M. & Mänttäri, I. 2005. Pukala intrusion, its age and connection hydrothermal alteration in Orivesi, southwestern Finland. Bulletin of the Geological Society of Finland 77, 165–180.

Talikka, M. 2007. Tectonic evolution of the Paleoprotezoic Tampere Belt during the Svecofennian orogeny, with reference to hydrothermal alteration at Kutemajärvi. In: Kojonen, K. et al. (eds.) Au-Ag telluride-selenide deposits. Geological Survey of Finland, Guide 53, 71–77.

Vaasjoki, M., Korsman, K. & Koistinen, T. 2005 Overview. In: Lehtinen, M., Nurmi, P. & Rämö, O.T. (eds.) Precambrian Geology of Finland – Key to the Evolution of the Fennoscandia Shield. Elsevier, Amsterdam, pp. 1–18.

Väisänen, M., Mänttäri, I. & Hölttä, P. 2002. Svecofennian magmatic and metamorphic evolution in southwestern Finland as revealed by U-Pb zircon SIMS geochronology. Precambrian Research 116, 111–127.

Virkkunen, M. 1962. Pegmatiittitutkimukset Tammelan ja Someron alueilla, Geological Survey of Finland, Report M17/Tm, So-62/1/85, 57 p. (in Finnish)

Yavuz, F., Yavuz, V. & Sasmaz, A. 2006. WinClastour – a Visual Basic program for tourmaline formula calculation and classification. Computers & Geosciences 32, 1156–1168.